HAL
open science

A quasi-monomode guided atom-laser from an all-optical Bose-Einstein condensate

A. Couvert, M. Jeppesen, T. Kawalec, G. Reinaudi, Renaud Mathevet, David Guéry-Odelin

To cite this version:

A. Couvert, M. Jeppesen, T. Kawalec, G. Reinaudi, Renaud Mathevet, et al.. A quasi-monomode guided atom-laser from an all-optical Bose-Einstein condensate. EPL - Europhysics Letters, 2008, 83, pp.50001. 10.1209/0295-5075/83/50001 . hal-00257245v2

HAL Id: hal-00257245

https://hal.science/hal-00257245v2

Submitted on 15 Sep 2008

HAL is a multi-disciplinary open access archive for the deposit and dissemination of scientific research documents, whether they are published or not. The documents may come from teaching and research institutions in France or abroad, or from public or private research centers.

L'archive ouverte pluridisciplinaire **HAL**, est destinée au dépôt et à la diffusion de documents scientifiques de niveau recherche, publiés ou non, émanant des établissements d'enseignement et de recherche français ou étrangers, des laboratoires publics ou privés.

A quasi-monomode guided atom-laser from an all-optical Bose-Einstein condensate

A. Couvert[1], M. Jeppesen[1,2] , T. Kawalec[1], G. Reinaudi[1], R. Mathevet[3] and D. Guéry-Odelin[1,3]

[1] *Laboratoire Kastler Brossel, CNRS UMR 8852, Ecole Normale Supérieure, 24 rue Lhomond, 75005 Paris, France*
[2] *Australian Centre for Quantum Atom Optics, Physics Department, The Australian National University, Canberra, 0200, Australia*
[3] *Laboratoire Collisions Agrégats Réactivité, CNRS UMR 5589, IRSAMC, Université Paul Sabatier, 118 Route de Narbonne, 31062 Toulouse CEDEX 4, France.*

PACS 03.75.Pp – Atom lasers
PACS 03.75.Mn – Multiple component condensates; spinor condensate
PACS 37.10.Gh – Atom traps and guides

Abstract. - We report the achievement of an optically guided and quasi-monomode atom laser, in all spin projection states ($m_F = -1$, 0 and $+1$) of $F = 1$ in rubidium 87. The atom laser source is a Bose-Einstein condensate (BEC) in a crossed dipole trap, purified to any one spin projection state by a spin-distillation process applied during the evaporation to BEC. The atom laser is outcoupled by an inhomogenous magnetic field, applied along the waveguide axis. The mean excitation number in the transverse modes is $\langle n \rangle = 0.65 \pm 0.05$ for $m_F = 0$ and $\langle n \rangle = 0.8 \pm 0.3$ for the low field seeker $m_F = -1$. Using a simple thermodynamical model, we infer from our data the population in each excited mode.

When atoms are coherently extracted from a Bose-Einstein condensate (BEC) they form an atom laser, a coherent matter wave in which many atoms occupy a single quantum mode. Atom lasers are orders of magnitude brighter than thermal atom beams, and are first and second order coherent [1, 2]. They are of fundamental interest, for example, for studies of atom-light entanglement, quantum correlations of massive particles [3] and quantum transport phenomena [4–10]. They are of practical interest for matter-wave holography through the engineering of their phase [11], and for atom interferometry because of their sensitivity to inertial fields [12].

Many prospects for atom lasers depend upon a high degree of control over the internal and external degrees of freedom and over the flux. The control of the output flux in a pulsed or continuous manner has been investigated using different outcoupling schemes: short and intense radiofrequency pulses [13], gravity induced tunneling [14], optical Raman pulses [15], long and weak radiofrequency fields [16], and by decreasing the trap depth [17].

The control of their internal state is intimately related to the outcoupling strategy. Atoms are either outcoupled in the magnetically insensitive (to first order) Zeeman state $m_F = 0$ or another Zeeman state, each offering different advantages. Atom lasers in $m_F = 0$ are ideal for precision measurement [18] because of their low magnetic sensitivity. Atoms in other Zeeman states, however, are ideal for measurements of magnetic fields because of their high magnetic sensitivity [19].

The control of the external degrees of freedom has been investigated through the atom laser beam divergence while propagating downwards due to gravity [20, 21]. Inhomogeneous magnetic field have been used to realize atom optical elements [22]. Recently, a guided and quasi-continuous atom laser from a magnetically trapped BEC has been reported [23].

In this Letter, we report on a new approach to generate guided atom laser. This method can produce an atom laser in *any* Zeeman state. In addition, our non-state changing outcoupling scheme leads to an intrinsically good transverse mode-matching, that enables the production of a *quasi-monomode* guided atom laser. Therefore, we achieve simultaneously a high degree of control of the internal and external degrees of freedom.

The atom laser is extracted from a Bose Einstein condensate produced in a dipole trap. The trap is made from a Ytterbium fiber laser (IPG LASER, model YLR-300-LP) with a central wavelength of 1072 nm and a

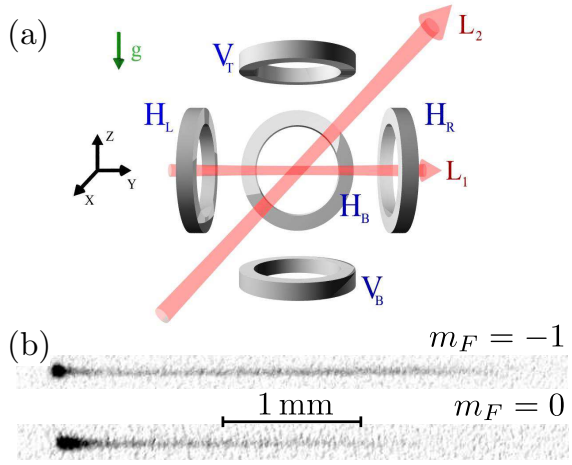

Fig. 1: (Colour online). (a) Schematic of experiment, showing trapping lasers and magnetic coils. The cross dipole optical trap is formed by two lasers of wavelength $\lambda = 1.07\,\mu$m, one horizontal (L_1) and one at 45° (L_2). The coils are used individually to produce magnetic field gradients: during the evaporation ramp, the top coil V_T is used for production of $m_F = +1$ condensates, the bottom coil V_B for $m_F = -1$, and the off-axis horizontal coil H_B for $m_F = 0$. Atom laser outcoupling is done with either on-axis coil, H_L or H_R. (b) Absorption images for $m_F = -1$ and $m_F = 0$ atom lasers in waveguides, taken after a 15 ms expansion time.

FWHM linewidth of 4 nm. We have used an intersecting beams configuration, formed by two focused linearly polarized beams: beam (L_1) is horizontal and has a waist of $w_1 \simeq 40\,\mu$m, and beam (L_2) which is in the $y-z$ plane at a 45 degree angle with respect to the horizontal beam, and a waist of $w_2 \simeq 150\,\mu$m (see fig. 1(a)).

In order to control the laser power P_i ($i = 1, 2$) of each beam, we used the first-order diffracted beam from water-cooled acousto-optic modulators, made in fused silica and designed for high power lasers. The selected diffraction order ensures that beam (L_1) and (L_2) have a frequency difference of 80 MHz. We actively stabilized the pointing of the vertical beam, and passively stabilized the pointing of the horizontal beam to less than 50 μrad.

The experimental sequence begins by collecting around 10^9 atoms of ^{87}Rb, in an elongated magneto-optical trap (MOT), loaded from a Zeeman slower source in less than 2 seconds. The elongated shape of the MOT results from the two-dimensional magnetic field gradient configuration. The dipole trap is on during the MOT loading, with powers $P_1 = 24$ W and $P_2 = 96$ W. To maximize the loading of atoms into the dipole trap, the horizontal beam L_1 is overlapped on the long axis of the MOT, and provides a reservoir of cold atoms [24]. In addition, we favor the selection of atoms in the hyperfine level $5S_{1/2}, F = 1$ by removing the repump light in the overlapping region, similar to the dark MOT technique [25].

To evaporate, we switch off the MOT and we reduce the power in each beam by typically two orders of magnitude, following the procedures shown in Ref. [26], and we produce spinor condensates of around 10^5 atoms[1]. The entire experimental cycle is less than six seconds.

To analyze the properties of the condensate, we use low-intensity absorption imaging, with a variable time-of-flight (TOF), after switching off the dipole beams. In addition, we can use the Stern and Gerlach effect by applying a magnetic field gradient during the expansion to spatially separate the spin components.

When evaporating with no magnetic field, we produce a condensate with an approximately equal number of atoms in each m_F spin state. To produce the atom laser, we require a BEC of one pure spin state. To do this, we use a single magnetic coil to produce a gradient in the magnetic field amplitude $\nabla|\mathbf{B}|$, and hence a force on the atoms due to the Zeeman effect. At the location of the atoms, this force is almost purely in one direction, along the axis of whichever coil is being used. We use such a force, perpendicular to the guide axis (L_1), to produce a spin-polarized BEC of an arbitrary m_F state.

Spin distillation to one m_F state occurs because, when the force is applied during evaporation, the trap is less deep for the other m_F states (see Inset of fig. 2), and they are evaporated first [17]. For example, to purify $m_F = 0$, we use the horizontal coil H_B (see fig. 1(a)), which forces the other m_F states out of the trap, attracting the $m_F = +1$ and repelling the $m_F = -1$ [27]. To purify $m_F = -1$, we use the bottom coil V_B, which partially cancels the effect of gravity for $m_F = -1$, has little effect on $m_F = 0$, and increases the effect of gravity for $m_F = +1$. Because atoms in the selected spin state are sympathetically cooled by the other atoms, the evaporation is more efficient, and we can produce condensates with a number of atoms in a given spin state approximatively three times greater than when evaporating with no field. We have confirmed that the three spin states are approximately at the same temperature during the entire evaporation. In fig. 2, we show the evolution of each spin state population in the course of evaporation for a spin distillation to the $m_F = 0$ state. From the slope of the evaporation trajectories in the number of atoms - temperature plot, we infer (using the evaporation model of Ref. [26]) that during the last second of evaporation, the ratio between trap depth and temperature η is 5.1 for $m_F = 0$ an 4.6 for $m_F = \pm 1$, which is further evidence for sympathetic cooling.

We demonstrate in the following that a BEC in a pure spin state held in an optical trap can be coupled to the horizontal arm of the trap in a very controlled manner, using magnetic forces along the guide axis. The large Rayleigh length (5 mm for the horizontal beam L_1) of the laser we use for the trap enables us to guide the atom laser over several millimeters (see fig. 1(b)). The data reported on

[1] For $m_F = 0$ (respectively $m_F = -1$) spin state experiments, the horizontal beam has a final power of 100 mW (respectively 85 mW) at the end of the evaporation, and the vertical beam a final power of 9.77 W (respectively 9.54 W).

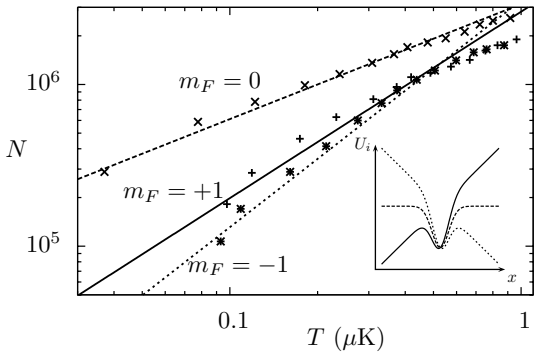

Fig. 2: Spin distillation. Number of atoms in each spin state versus temperature during the evaporation process, showing the sympathetic cooling and purification of $m_F = 0$ down to degeneracy. The purification is due to a horizontal magnetic field gradient, applied during the evaporation ramp. This field induces a force on $m_F = \pm 1$ that reduces the effective depth that they experience (see inset, U_i is the potential experienced by an atom in a m_i Zeeman sublevel ($i = -1, 0, +1$)).

in this letter are for the $m_F = 0$ and the $m_F = -1$ spin states. Similar results have been obtained with $m_F = +1$ state, using the same sequence as for $m_F = -1$ but with the magnetic fields reversed.

After the evaporation is complete, we prepare to outcouple the atom laser by linearly *increasing* over 200 ms the power in the horizontal beam to 200 mW for $m_F = \pm 1$ (resp. 400 mW for $m_F = 0$) and *decreasing* the power in the vertical beam to 1 W for $m_F = \pm 1$ (resp. 800 mW for $m_F = 0$). This is done so that the maximum available magnetic force will be sufficient to outcouple. At the same time, we linearly increase a magnetic gradient along the horizontal guide axis from 0 to 0.18 T/m, to reach the threshold of outcoupling. Finally, to outcouple we hold the power in each beam constant and increase the magnetic gradient from 0.18 T/m to 0.22 T/m over a further 200 ms to generate the beam. For atoms in $m_F = 0$ state, the force exerted by the magnetic field is weaker than the one experienced by atoms in $m_F = \pm 1$, since it relies on the second order Zeeman effect. Nevertheless, we have demonstrated this magnetic outcoupling method for all three spin states.

The role played by the magnetic field is two fold: (i) it lowers the trap depth along the optical guide axis and favors the progressive spilling of atoms, and (ii) it accelerates the atoms coupled into the guide, similar to gravity for standard non guided atom lasers. Note that unlike gravity, we can control and even turn off this inhomogeneous magnetic field at will.

The figure of merit for a guided atom beam is the number of transverse modes that are populated. Experimentally, we cannot measure directly those populations, but we have access to the mean excitation number of the transverse modes $\langle n \rangle$. Using the virial theorem for a non interacting beam[2] in a harmonic guide, one can show that the transverse velocity dispersion Δv obeys:

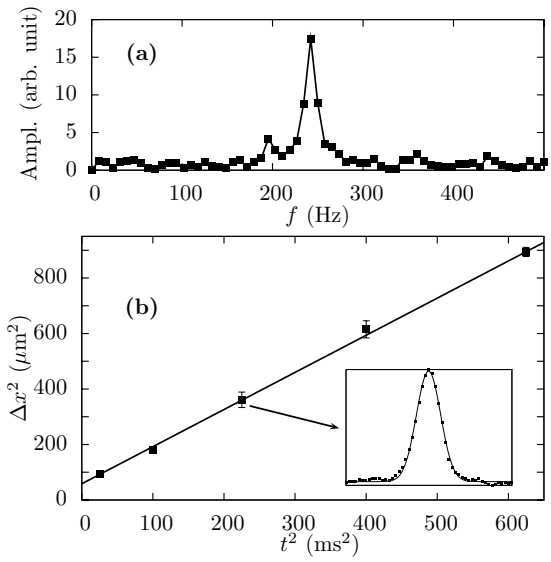

Fig. 3: Measurements of the trapping frequency and the velocity dispersion for rubidium atoms in $|F = 1, m_F = 0\rangle$. (a) Fourier transform of atom cloud oscillations in the waveguide. The peak has a frequency of 245 Hz and a width of 10 Hz. (b) Plot of measurements of $(\Delta x(t))^2$ against t^2 for the time of flight expansion of the atom laser, and the straight line fit to the data, from which we infer the velocity dispersion $\Delta v = 1.2$ mm/s. Inset: Example of Gaussian fit to integrated data, for a 15 ms TOF.

$$\frac{1}{2} m (\Delta v)^2 = \frac{\hbar \omega_z}{2} \left(\langle n \rangle + \frac{1}{2} \right). \quad (1)$$

To infer $\langle n \rangle$, one needs to measure Δv and ω_z. The trap frequency ω_z of the optical guide is determined by observing the centre of mass oscillation of an atom cloud prepared at this location. The transverse excitation is produced by giving a momentum kick with a pulsed magnetic field. fig. 3(a) shows the Fourier transform of the oscillations from which we infer a trap frequency of $\omega_z = 2\pi \times (245 \pm 10)$ Hz. The same method gives a trap frequency of 170 Hz for the experimental conditions used to investigate atom lasers in the internal state $|F = 1, m_F = 1\rangle$.

The velocity dispersion Δv is inferred from a TOF measurement. We integrate the absorption images along the atom laser propagation direction over one millimeter *i.e.* on a distance over which the transverse frequency is constant to within a few percent. The resulting one dimensional profiles are fitted with a Gaussian function to find the width $\Delta x(t)$, t being the TOF duration. We then find Δv through the relation $(\Delta x(t))^2 = (\Delta x_0)^2 + (\Delta v)^2 t^2$. A typical fit and TOF measurement can be seen in fig. 3(b).

[2]The outcoupled beam is in the low density regime $\rho a \leq 0.1 < 1$, where a is the scattering length and ρ the linear density [4, 5].

Using Eq. 1, we find $\langle n \rangle = 0.8 \pm 0.3$ for a guided atom laser of atoms in the $m_F = -1$ state, and $\langle n \rangle = 0.65 \pm 0.05$ for the $m_F = 0$ state[3]. From our data, we conclude that this quality is preserved as the beam propagates in the optical guide over several millimeters. We have therefore produced a quasi-monomode guided atom laser for any Zeeman state. Before analyzing in more detail the transverse mode distribution, we discuss the issue of the flux of the laser beam.

The control of the output flux is also a crucial issue for most applications. Its variation as a function of time can be extracted from the absorption images of fig. 1(b). Those images are taken after a 15 ms time of flight in absence of any magnetic force. An atom that experiences the mean acceleration $\bar{a}$ ($= \mu_B b/2m$ for an $m_F = -1$ atom) where $b = 20$ T/m during a time τ, is located after a time-of-flight of duration t at $y - y_0 = \bar{a}\tau^2/2 + \bar{a}\tau t$, where y_0 is the point of outcoupling. From the absorption images we have a direct access to the mean linear atomic density $\rho[y]$ along the propagation axis. The flux is thus given by[4]: $\Phi(\tau) = \rho[y(\tau)](\mathrm{d}y/\mathrm{d}\tau)$. We have shown in fig. 4 two examples of the flux as a function of time, deduced from the measured density in the absorption images of a guided atom laser in $m_F = 0$ and in $m_F = -1$. For the $m_F = 0$ state, the flux increases over the 30 first milliseconds to 4×10^5 atoms/s, and then remains constant over more than 70 ms. For the $m_F = -1$ state, a flux up to 7×10^5 atoms/s is reached in just 20 ms. The flux decreases afterwards as the BEC get depleted. For our experimental sequence, the magnetic force is smaller for the $m_F = 0$ state compared to $m_F = -1$ state, and the smaller outcoupling rate yields a nearly constant output flux for $m_F = 0$. During the outcoupling process, the flux is determined by the chemical potential which is equal to the trap depth. Therefore, to have the flux constant and stable over a long period of time would require precise control of each beam's power and position, and of the magnetic field gradient, all over the entire outcoupling.

The linear density ρ extracted from our data ranges from 5×10^7 to 10^7 atoms/m. We propose in the following a simple model that gives the whole excitation spectrum for the transverse degrees of freedom from the experimental values of the linear density ρ and the mean excitation number $\langle n \rangle$. The beam is assumed to be a perfect Bose gas at thermodynamical equilibrium made of N atoms confined longitudinally by a box of size $L = N/\rho$ with periodic boundary conditions and transversally by a harmonic potential of angular frequency ω. The one-particle eigenstates of the system are then labelled by three integers: the non-negative integers n_X and n_Z labelling the eigenstates of the harmonic oscillator along the transverse X and Z axis, and the integer ℓ_Y labelling the momentum along Y. Replacing in the large L limit the sum over ℓ_Y by an integral, the normalization condition reads:

$$\rho\lambda = g_{1/2}(z) + \sum_{p=1}^{\infty} \frac{z^p}{p^{1/2}} \left(\frac{1}{(1-e^{-p\xi})^2} - 1 \right), \qquad (2)$$

where we have introduced the de Broglie wavelength $\lambda = \hbar/(2\pi m k_B T)^{1/2}$, the fugacity $z = \exp(\beta\mu)$, the dimensionless parameter $\xi = \beta\hbar\omega_z$ and the $p = 1/2$ Bose function $g_{1/2}(z) = \sum_{n=1}^{\infty} z^n/n^{1/2}$. Note that the function $g_{1/2}(z)$ is not bounded when $z \to 1$, which means physically that, in our trapping geometry, there is no Bose Einstein condensation in the thermodynamical limit defined as $L, N \to \infty$ with a fixed linear density $\rho = N/L$. However, in such a combined box+harmonic confinement, Bose Einstein condensation in the *transverse* ground state level does occur at thermodynamical equilibrium [28]. The expression for the critical temperature is :

$$T_c = \frac{\hbar\omega}{k_B} \left(\frac{\rho\lambda}{\zeta(5/2)} \right)^{1/2}, \qquad (3)$$

with $\zeta(5/2) \simeq 1.34$.

The mean excitation number $\langle n \rangle$ is obtained by calculating the transverse energy $E_\perp = 2N\hbar\omega\langle n \rangle$. We find:

$$\langle n \rangle = \frac{1}{\rho\lambda_0\xi^{1/2}} \sum_{p=1}^{\infty} \frac{z^p}{p^{1/2}} \frac{e^{-p\xi}}{(1-e^{-p\xi})^3}, \qquad (4)$$

with $\lambda_0 = \hbar/(2\pi m\hbar\omega)^{1/2}$. From Eqs. (2) and (4) and the experimental measurements of $\langle n \rangle$ and ρ, we determine numerically the dimensionless parameters ξ and z that allows one to infer all the equilibrium properties of the Bose gas. As an example, the occupation numbers P_k of all transverse energy states $\epsilon_k = k\hbar\omega$ are given by:

$$P_k = \frac{1}{\rho\lambda}(k+1) g_{1/2}\left(z e^{-k\xi}\right), \qquad (5)$$

where the $(k+1)$ factor accounts for the degeneracy of the state k. For our data with a linear density equal to $\rho = 5\times10^7$ atoms/m and $\langle n \rangle \simeq 0.7$, we find 50 % of atoms in the transverse ground state and a temperature of 20 nK, well below the critical temperature of 60 nK obtained for this linear density according to Eq. 3. The same calculation yields 14% of atoms in the transverse ground state for the parameters and data reported in Ref. [23] where $\langle n \rangle \simeq 2.0$ (see Fig 5). The thermodynamical equilibrium assumption made in the previous reasoning is approximately valid for the data presented in this letter. Indeed, we have estimated that each atom undergoes a few collisions after being outcoupled from the Bose Einstein condensate.

The atomic intensity fluctuations of the atom laser beam are related to the dimensionless parameter $\chi = \hbar^2\rho^3 g/(m k_B^2 T^2)$, where $g = g_{3D}/(2\pi a_0^2)$ with $g_{3D} =$

[3]The larger error bar for the $m_F = -1$ state might be attributed to a higher sensitivity to technical noises due to the lower guide frequencies.

[4]The classical reasoning performed here is justified since the length scales of interest are much larger than the quantum length $\ell = (\hbar^2/m^2\bar{a})^{1/3} < 1$ μm on which the Airy-like wave function oscillates.

$4\pi\hbar^2 a/m$, a being the scattering length and $a_0 = (\hbar/m\omega_{z,x})^{1/2}$ [29]. For $\chi \gg 1$, small atomic intensity fluctuations are expected, and conversely for $\chi \ll 1$. With our parameters, the decrease of the atomic density as the atom laser propagates yields a decrease of χ from 100 to 1 in 100 ms. An interesting prospect, with a better imaging system, deals with the study of atomic intensity fluctuations and the investigation of the longitudinal coherence with guided atom lasers produced in different interacting regimes, including out-of-thermal equilibrium states.

Two effects are probably involved in the residual multimode character of our atom laser. First, the residual thermal fraction in equilibrium with condensate in the trap can populate the excited transverse modes. Second, slight shaking of the position of the relative position of beams (L_1) and (L_2) during the outcoupling process can result in an increase value of the mean excitation number. We therefore envision two main improvements for future experiments: (i) a position locking scheme for the guide with a bandwidth of a few kHz, and (ii) a more adiabatic outcoupling by shaping the ramp of the magnetic field, which would require a numerical optimization by solving the three-dimensional Gross-Pitaevskii equation.

In conclusion, we have succeeded in smoothly coupling an optically trapped BEC to a horizontal optical guide with low transverse excitation. The near monomode nature of the atom laser will be important in all applications which use phase engineering such as matter-wave holography [30]. A guided atom laser is an ideal tool to investigate the transmission dynamics of coherent matter waves through different structures. Such studies have their counterpart in electronic transport phenomena, including the generalization to cold atoms of Landauer's theory of conductance [31], the atom-blockade phenomenon [6–8], non-linear resonant transport [9, 10]. Guided atom lasers in magnetically sensitive states are ideal to combine with magnetic structures, such as on atom-chips [32].

Finally, we emphasize that this work, combined with a continuous replenishing of the optical dipole trap [33], can be viewed as a promising strategy to generate a continuous guided atom laser.

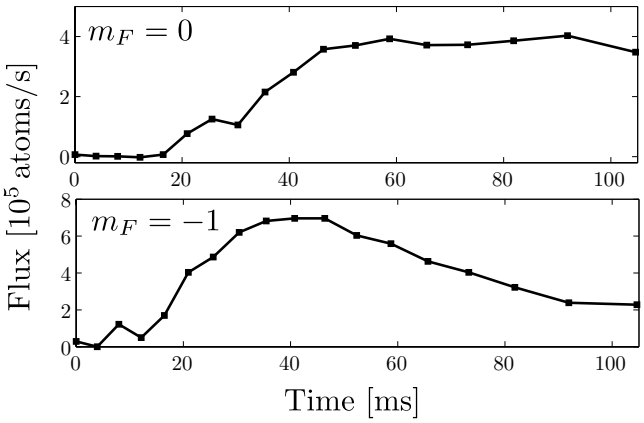

Fig. 4: Flux of atom laser versus time for the guided atom lasers depicted in fig. 1(b), in the $m_F = 0$ and $m_F = -1$ spin states (a binning procedure has been used to smooth out the noise due to the CCD camera).

* * *

We thank C. Cohen-Tannoudji, J. Dalibard, Y. Castin and I. Carusotto for useful comments and fruitful discussions. Support for this research came from the Délégation Générale pour l'Armement (DGA, contract number 05-251487), the Institut Francilien de Recherche sur les Atomes Froids (IFRAF) and the Plan-Pluri Formation (PPF) devoted to the manipulation of cold atoms by powerful lasers. G. R. acknowledges support from the DGA, and M. J. from IFRAF.

REFERENCES

[1] Bloch I., Hänsch T. and Esslinger T., *Nature*, **403** (2000) 166.
[2] Öttl A., Ritter S., Köhl M. and Esslinger T., *Phys. Rev. Lett.*, **95** (2005) 090404.
[3] Haine S. A., Olsen M. K. and Hope J. J., *Phys. Rev. Lett.*, **96** (2006) 133601.
[4] Leboeuf P. and Pavloff N., *Phys. Rev. A*, **64** (2001) 033602.
[5] Pavloff N., *Phys. Rev. A*, **66** (2002) 013610.
[6] Carusotto I. and La Rocca G. C., *Phys. Rev. Lett.*, **84** (2000) 399.
[7] Carusotto I., *Phys. Rev. A*, **63** (2001) 023610.
[8] Carusotto I., Embriaco D. and La Rocca G. C., *Phys. Rev. A*, **65** (2002) 053611.
[9] Paul T., Richter K. and Schlagheck P., *Phys. Rev. Lett.*, **94** (2005) 020404.
[10] Paul T., Leboeuf P., Pavloff N., Richter K. and Schlagheck P., *Phys. Rev. A*, **72** (2005) 063621.
[11] Olshanii M., Dekker N., Herzog C. and Prentiss M., *Phys. Rev. A*, **62** (2000) 033612.
[12] Berman P., (Editor) *Atom interferometry* (Academic Press, San Diego) 1997.
[13] Mewes M.-O., Andrews M. R., Kurn D. M., Durfee D. S., Townsend C. G. and Ketterle W., *Phys. Rev. Lett.*, **78** (1997) 582.
[14] Anderson B. P. and Kasevich M. A., *Science*, **282** (1998) 1686.
[15] Hagley E. W., Deng L., Kozuma M., Wen J., Helmerson K., Rolston S. L. and Phillips W. D., *Science*, **283** (1999) 1706.
[16] Bloch I., Hänsch T. W. and Esslinger T., *Phys. Rev. Lett.*, **82** (1999) 3008.
[17] Cennini G., Ritt G., Geckeler C. and Weitz M., *Phys. Rev. Lett.*, **91** (2003) 240408.
[18] Gill P., (Editor) *Proceedings of the 6th Symposium on Frequency Standards and Metrology* (World Scientific) 2002.
[19] Vengalattore M., Higbie J. M., Leslie S. R., Guzman J., Sadler L. E. and Stamper-Kurn D. M., *Phys. Rev. Lett.*, **98** (2007) 200801.
[20] Riou J.-F., Guerin W., Le Coq Y., Fauquembergue

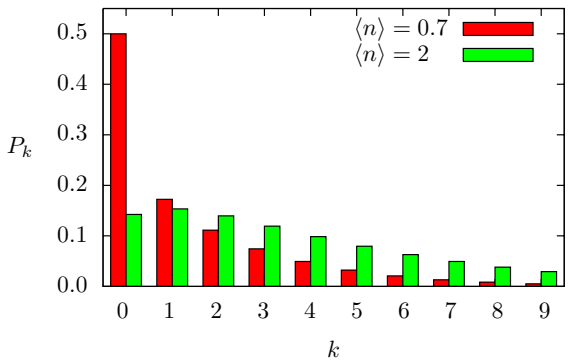

Fig. 5: (Colour online). Transverse excitation spectrum. Measuring the linear atomic density and the mean excitation number $\langle n \rangle$, one can infer the distribution of the transverse energy states $\epsilon_k = k\hbar\omega$ using a thermodynamical equilibrium approach where the atom laser beam is modelled by a Bose gas confined by a box longitudinally and an harmonic potential transversally. For a linear density equal to 5×10^7 atoms/m, the occupation number of the ground state is on the order of 50 % for our data where we measure $\langle n \rangle \simeq 0.7$, and 14% when $\langle n \rangle \simeq 2.0$ as reported in Ref. [23].

M., Josse V., Bouyer P. and Aspect A., *Phys. Rev. Lett.*, **96** (2006) 070404.

[21] Jeppesen M., Dugué J., Dennis G. R., Johnsson M. T., Figl C., Robins N. P. and Close J. D., *Phys. Rev. A*, **77** (2008) 063618.

[22] Bloch I., Köhl M., Greiner M., Hänsch T. W. and Esslinger T., *Phys. Rev. Lett.*, **87** (2001) 030401.

[23] Guerin W., Riou J.-F., Gaebler J. P., Josse V., Bouyer P. and Aspect A., *Phys. Rev. Lett.*, **97** (2006) 200402.

[24] Takasu Y., Honda K., Komori K., Kuwamoto T., Kumakura M., Takahashi Y. and Yabuzaki T., *Phys. Rev. Lett.*, **90** (2003) 023003.

[25] Ketterle W., Davis K. B., Joffe M. A., Martin A. and Pritchard D. E., *Phys. Rev. Lett.*, **70** (1993) 2253.

[26] O'Hara K. M., Gehm M. E., Granade S. R. and Thomas J. E., *Phys. Rev. A*, **64** (2001) 051403.

[27] Lundblad N., Thompson R. J., Aveline D. C. and Maleki L., *Opt. Express*, **14** (2006) 10164.

[28] Mandonnet E., Minguzi A., Dum R., Carusotto I., Castin Y. and Dalibard J., *Eur. Phys. J. D*, **10** (2000) 9.

[29] Castin Y., *J. Phys. IV France*, **116** (2004) 89.

[30] Fujita J., Mitake S. and Shimizu F., *Phys. Rev. Lett.*, **84** (2000) 4027.

[31] Thywissen J. H., Westervelt R. M. and Prentiss M., *Phys. Rev. Lett.*, **83** (1999) 3762.

[32] Reichel J., *Applied Physics B: Lasers and Optics*, **74** (2002) 469.

[33] Chikkatur A. P., Shin Y., Leanhardt A. E., Kielpinski D., Tsikata E., Gustavson T. L., Pritchard D. E. and Ketterle W., *Science*, **296** (2002) 2193.